Available online at www.sciencedirect.com
ScienceDirect
Journal of Molecular Catalysis A: Chemical 266 (2007) 55–64
JOURNAL OF MOLECULAR CATALYSIS A: CHEMICAL
www.elsevier.com/locate/molcata

Study of the reaction mechanisms between Sn-(n-C_4H_9)$_4$ and alumina surface sites Application to the controlled preparation of $PtSn/Al_2O_3$ catalysts

M. Womes [a,*], F. Le Peltier [a,1], S. Morin [a,2], B. Didillon [a], J. Olivier-Fourcade [b], J.C. Jumas [b]

[a] *Institut Français du Pétrole, 1&4 Avenue de Bois Préau, B.P. 311, 92506 Rueil-Malmaison, France*
[b] *Laboratoire des Agrégats Moléculaires et Matériaux Inorganiques (UMR 5072 CNRS), Université Montpellier II, CC 15, Place E. Bataillon, 34095 Montpellier Cedex 5, France*

Received 25 September 2006; received in revised form 17 October 2006; accepted 18 October 2006
Available online 24 October 2006

Abstract

The reaction mechanisms between Sn-(n-C_4H_9)$_4$ and several specific types of surface sites on alumina are studied. A surface treatment is described allowing the complete elimination of reactive surface sites and avoiding the anchoring of Sn-(n-C_4H_9)$_4$ on the support. This surface deactivation is applied to the preparation of bimetallic $PtSn/Al_2O_3$ catalysts by controlled selective decomposition of Sn-(n-C_4H_9)$_4$ on the reduced metallic particles of a Pt/Al_2O_3 catalyst. The resulting bimetallic particles are analysed by ^{119}Sn Mössbauer spectroscopy at different stages of the preparation procedure. The tin anchoring sites on the platinum particles are identified on the basis of their specific Mössbauer hyperfine parameters. Tin atoms in contact with the support or with platinum are distinguished from those enclosed in bulk-SnO_2-like agglomerates. A structural model is proposed describing at an atomic scale the morphology of the bimetallic particles and their evolution under various heat treatments. The results are compared with those of a catalyst prepared by conventional impregnation methods on a not specifically pretreated support.

Keywords: Alumina surface sites; Reaction mechanisms Sn-(n-C_4H_9)$_4$–alumina surfaces; Controlled surface reaction; $PtSn/Al_2O_3$ catalysts; ^{119}Sn Mössbauer spectroscopy

1. Introduction

Bimetallic $PtSn/Al_2O_3$ catalysts are currently widely used in the principal processes of catalytic transformation of hydrocarbons for automotive or petrochemical purposes [1–8]. Their importance for the production of automotive gasoline lies in their ability to catalyse dehydrogenation, isomerisation and dehydrocyclisation (aromatisation) reactions and to increase in this way the gasoline octane number [1–5]. In the production of fine chemicals the preparation of unsaturated alcohols by selective hydrogenation of α,β-unsaturated aldehydes has great industrial importance [6–8]. The introduction of bimetallic catalysts has been an important step in the improvement of the selectivity and stability of reforming catalysts. The presence of a second metal, such as tin, reduces considerably the deactivation of the catalyst by coke formation and coalescence of the metallic particles during the reaction and regeneration steps, respectively [9]. Two positive effects are associated with the presence of tin: (i) a steric effect, caused by dilution of surface platinum atoms (*i.e.* tin decreases the size of platinum ensembles constituting the catalytically active sites) [10,11] and (ii) an electronic effect, caused by influencing the electronic density on platinum atoms and thereby modifying their bonding properties [12]. It is obvious that improvements with respect to monometallic catalysts are only achieved if the two metals are in close contact. Co-

* Corresponding author. Present address: Laboratoire des Agrégats Moléculaires et Matériaux Inorganiques (UMR 5072 CNRS), Université Montpellier II, CC 15, Place E. Bataillon, 34095 Montpellier Cedex 5, France.
Tel.: +33 4 67 14 45 48; fax: +33 4 67 14 33 04.
E-mail address: womes@univ-montp2.fr (M. Womes).
[1] Present address: Axens, 89 Boulevard Franklin Roosevelt, B.P. 50802, 92508 Rueil-Malmaison Cedex, France.
[2] Present address: IFP-Lyon, B.P. 3, 69390 Vernaison, France.

1381-1169/$ – see front matter © 2006 Elsevier B.V. All rights reserved.
doi:10.1016/j.molcata.2006.10.040

impregnation techniques consisting of impregnating the support simultaneously by platinum and tin precursors [13,14] do not necessarily lead to the formation of bimetallic agglomerates. Alternative methods have therefore been developed based on the principle of controlled surface reactions (CSR), which make use of the selective anchoring of an organometallic tin complex, like tin-tetraalkyls Sn-R_4, on reduced metal particles of a monometallic parent catalyst [15,16] following the equation:

$$x(M_s\text{-}H) + Sn\text{-}R_4 \rightarrow xM_s\text{-}Sn\text{-}R_{4-x} + xR\text{-}H$$

where M_s denotes a surface metal atom like platinum [15] or rhodium [16]. Since then, numerous studies have been devoted to the preparation of bimetallic catalysts by CSR on Al_2O_3 [17,18] as well as on SiO_2 [19–22].

However, this method is not automatically safe insofar as undesired anchoring on highly reactive surface sites of the support can occur. These sites are surface ions which are coordinatively unsaturated (c.u.s.) due to the treatments the support has been exposed to before, like calcinations having partially dehydroxylated the surface or any step of the production process having led to a defective surface structure. C.u.s. aluminium and oxygen ions act as strong Lewis acid and base sites, respectively. Dehydroxylation of an alumina surface covered by a complete monolayer of OH-groups is usually described as a condensation of neighbouring hydroxyl groups to form H_2O molecules [23–25]. The c.u.s. sites progressively formed in this way upon heating are arranged in a rather regular way up to 300 °C. Further dehydroxylation at higher temperatures creates various types of new c.u.s. sites with lower coordination number and domains containing several neighbouring c.u.s. sites, all characterised by enhanced reactivity. A recent study of the interaction mechanisms between γ-alumina surfaces and platinum bis-acetylacetonate, $Pt(acac)_2$, has allowed distinguishing three types of surface sites on the basis of their specific reactivity towards $Pt(acac)_2$ [26]. Surface OH groups as the first type do not interact with $Pt(acac)_2$ and no adsorption takes place on completely hydroxylated surfaces. Partial dehydroxylation at temperatures up to 350 °C creates two further types of surface sites, one of lower reactivity (type A), interpreted as single, isolated c.u.s., on which $Pt(acac)_2$ is anchored by simple physisorption, and one of higher reactivity (type B), considered as single c.u.s. of lower coordination number than type A or as several neighbouring c.u.s., which induces a partial decomposition of the complex with loss of one acac-ligand, the remaining Pt-acac being chemically bonded to surface oxygen atoms. This same study has also demonstrated the possibility to completely eliminate the reactive sites A and B and to completely suppress any anchoring of the platinum complex on the support by applying appropriate surface treatments. In this way it became possible to anchor $Pt(acac)_2$ on the reduced platinum particles of a Pt/Al_2O_3 parent catalyst without any undesired side reaction.

The aim of the present work was to develop a corresponding preparation method for bimetallic catalysts, guaranteeing anchoring of a tin precursor exclusively on reduced platinum particles and avoiding undesired deposition on the support. A widely used precursor for the preparation of tin-containing catalysts is Sn-(n-C_4H_9)$_4$. The interaction mechanisms of this complex with SiO_2 surfaces have been studied in detail by several authors [20,27,28]. Little is known, however, about the way it reacts with alumina surfaces. Margitfalvi et al. pointed out that Sn-(n-C_4H_9)$_4$ reacts with surface OH groups on alumina [29,30], while no such side reaction was observed on silica [31]. Nothing seems to be known about interactions with c.u.s. surface sites. We thus performed a detailed study of the reaction mechanisms between this complex and, especially, the three types of surface sites identified in the previous work on $Pt(acac)_2$ [26]. The results of this study will be presented in the first part of the present paper. The following section describes the effect of a surface treatment similar to that developed in Ref. [26] regarding the efficient suppression of any anchoring of Sn-(n-C_4H_9)$_4$ on alumina and the controlled and exclusive anchoring of the complex on reduced platinum particles. Finally, we analyse bimetallic catalysts obtained in this way and compare them with samples prepared by other methods. This analysis is mainly focussed on the morphology of the bimetallic particles with the aim to identify the tin anchoring sites on the platinum particles and to establish a structural model of the bimetallic particles. Besides conventional experimental techniques like H_2/O_2 chemisorption to determine the fraction of surface atoms, we use here ^{119}Sn Mössbauer spectroscopy, which provides a local probe of the environment of the tin atoms on an atomic scale. The advantageous properties of the ^{119}Sn nucleus allow not only determining the tin valence state, Sn(IV), Sn(II) or metallic Sn(0), but also distinguishing for each of these valence states tin atoms in different environments regarding the local symmetry or the covalent or ionic character of the ligands. ^{119}Sn Mössbauer spectroscopy is therefore an ideal tool for the analysis of multiphased samples and was consequently applied in the field of catalysis by several authors [18,22,28,32,33]. Our interpretation of the present results is based on a recent exhaustive study of the various tin species occurring in Sn/Al_2O_3 and $SnPt/Al_2O_3$ samples as a function of the preparation method or the oxidation and reduction conditions [33].

2. Experimental

2.1. Sample preparation

Samples were prepared on pellets of γ_c-alumina of a diameter of 2 mm, a specific surface area of 200 m^2/g and a pore volume of 0.6 cm^3/g supplied by Axens.

2.1.1. Impregnation of alumina pellets with Sn-(n-C_4H_9)$_4$

Two kinds of surface pre-treatments were applied to alumina pellets prior to impregnation with Sn-(n-C_4H_9)$_4$ in order to study the interaction mechanisms between Sn(n-C_4H_9)$_4$ and alumina surface sites:

(i) Calcination of the support during 2 h at 623 K in a dry air stream, followed by cooling down to room temperature overnight in the same air stream. In the following, a support treated in this way will be referred to as a reactive support ("R").

(ii) Hydroxylation by incipient wetness impregnation with an amount of water corresponding to the pore volume of the pellets. The support was then dried at 393 K overnight. No calcination prior to the hydroxylation was carried out. These supports will be referred to as deactivated supports ("D").

These supports were impregnated with a solution of Sn(n-C_4H_9)$_4$ in heptane by an incipient wetness technique. The solvent volume was equal to the pore volume of the pellets, with an excess of 10% to take into account solvent evaporation during the impregnation procedure. The amount of Sn-(n-C_4H_9)$_4$ solvated corresponded to 0.50 wt.% Sn with respect to the support mass and was entirely deposited on the support as shown by X-ray fluorescence. The pellets were then dried at room temperature for several days and finely ground prior to acquisition of ^{119}Sn Mössbauer spectra.

2.1.2. Preparation of bimetallic $PtSn/Al_2O_3$ catalysts

The two metals were deposited in two separate steps, starting with platinum. The initial step of the preparation was a hydroxylation of the support surface as described above under (ii). This hydroxylation method does not lead to a complete elimination of all surface sites of low reactivity (type A), allowing in this way the physisorption of Pt(acac)$_2$ on the support. It further guarantees a homogeneous distribution of the platinum across the pellets [26]. The hydroxylated pellets were impregnated during 24 h at room temperature with a solution of Pt(acac)$_2$ (Johnson Matthey, >98.8%) in toluene, with a solvent to support ratio of 5 ml/g. The solution was slowly stirred to facilitate penetration of the pores. The sample was then filtered, washed in toluene, dried overnight at 393 K and finally calcined 2 h at 623 K in an air stream. This procedure led to catalysts with a high fraction of more than 80% of surface platinum atoms. Catalysts with a higher loading of platinum and a lower dispersion (45–55%) were obtained from these highly dispersed samples by the controlled anchoring of further Pt(acac)$_2$ on reduced platinum particles in a CSR as described in detail in Ref. [26].

Tin was anchored on these platinum catalysts by selective decomposition of Sn-(n-C_4H_9)$_4$ on the reduced platinum particles. To this end, the platinum catalysts were reduced 2 h under pure hydrogen at 723 K and then cooled under an argon stream. The necessary elimination of reactive surface sites mentioned in Section 1 was achieved by exposing the platinum catalysts to a stream of water-saturated nitrogen during 24 h at room temperature which, in contrast to the hydroxylation technique described in Section 2.1.1 under (ii), leads to a complete hydroxylation of the surface [26]. The samples were then again reduced in a dry hydrogen stream at room temperature for 1 h and transferred without any air exposure to a glass vessel used for impregnation. This vessel was filled with a solution of Sn-(n-C_4H_9)$_4$ (Merck) in n-heptane with a solvent to support ratio of 5 ml/g. A weak bubbling of argon (alternatively hydrogen in some cases) was maintained through the solution during the reaction. After 6 h of reaction at room temperature the samples were filtered, washed in heptane, dried, and calcined 1 h at 393 K, 1 h at 623 K and finally 1 h at 793 K in dry air.

2.1.3. Preparation of bimetallic $SnPt/Al_2O_3$ catalysts

As before, the two metals were deposited in two separate steps, now starting with tin. The support was hydroxylated as described in Section 2.1.1 under (ii) and then impregnated with a solution of Sn-(n-C_4H_9)$_4$ in n-heptane by an incipient wetness technique, using a solvent volume equal to the pore volume of the support with an excess of 10%. After calcination 1 h at 393, 623, and 793 K each, and after cooling down to room temperature, the tin impregnated support was again hydroxylated as under (ii) and dried at 393 K in air overnight. It was then immersed during 24 h in a solution of Pt(acac)$_2$ in toluene, using a solvent to support mass ratio of 5 ml/g. The sample was then filtered, washed in toluene, dried overnight at 393 K and finally calcined 2 h at 623 K in an air stream. This procedure involves no controlled surface reaction and platinum is expected to be mainly deposited on the support and not selectively on tin.

2.2. Sample characterisation

2.2.1. Metal loading

Platinum and tin contents were determined by X-ray fluorescence on a Philips PW 1480 apparatus.

2.2.2. Metal dispersion

Chemisorption experiments were carried out on a χ-Sorb apparatus (IFP licence). Catalysts were calcined at 623 K in dry air, cooled down to room temperature under the same air stream, reduced at 723 K and cooled down to room temperature under hydrogen. After elimination of all not-chemisorbed hydrogen by a stream of helium, the chemisorbed hydrogen was titrated by pulses of oxygen, supposing a stoichiometry of hydrogen to platinum of 1:1. A second titration was carried out after reduction by hydrogen at room temperature. For monometallic Pt/Al_2O_3 catalysts the results of both titrations agreed in all cases within experimental error. For bimetallic PtSn catalysts the second titration gives the fraction of surface Pt atoms alone while the oxygen uptake of the first titration cycle contains contributions from reduction and oxidation of both platinum and tin atoms [33]. From repeated measurements of the dispersion of a reference catalyst over a long time period we estimate the experimental error in all chemisorption results to ±2% dispersion absolute.

2.2.3. Mössbauer spectroscopy

^{119}Sn Mössbauer spectra were recorded in transmission geometry in the constant acceleration mode, using equipment supplied by Ortec and Wissel. Low temperature spectra were recorded by placing the sample in a helium flow cryostat. The nominal activity of the $Ba^{119m}SnO_3$ source was 10 mCi. The velocity scale was calibrated by means of a room temperature spectrum of α-Fe recorded with a ^{57}Co(Rh) source. The hyperfine parameters δ (isomer shift) and ΔE_q (quadrupole splitting) were determined by fitting Lorentzian lines to the experimental data by using the ISO programme [34]. Isomer shifts of samples studied in the present work are given with respect to the room

temperature spectrum of $BaSnO_3$. The error in the determination of the hyperfine parameters is ±0.06 mm/s.

3. Results and discussion

3.1. Interaction Sn(n-C_4H_9)$_4$–alumina surfaces

Two types of supports, one deactivated (D) and the other highly reactive (R), were impregnated with Sn-(n-C_4H_9)$_4$ as described in Section 2.1.1. The Mössbauer spectra of these samples, recorded at 16 K, are shown on Fig. 1b and c, respectively, together with the spectrum of pure Sn-(n-C_4H_9)$_4$ shown for comparison on Fig. 1a. The hyperfine parameters obtained for pure Sn-(n-C_4H_9)$_4$ (c.f. Table 1) are in good agreement with results published previously [28]. The isomer shift δ of 1.36 mm/s lies within the range of Sn(IV) compounds with rather covalent bonds, the zero quadrupole splitting ΔE_q reflects the perfect tetrahedral symmetry of the charge distribution around the tin nucleus.

Impregnation of a deactivated support with Sn-(n-C_4H_9)$_4$ leaves the tin complex intact, as can be seen from Fig. 1b and Table 1. The complex is anchored exclusively by physisorption. In contrast to this, two types of complexes are found on the reactive support, as shows the Mössbauer spectrum on Fig. 1c. The first is purely physisorbed Sn-(n-C_4H_9)$_4$ as on support D. The second is characterised by an important quadrupole splitting indicating a strong modification of the first co-ordination shell around tin. Comparison with the hyperfine parameters reported by Nédez et al. [28] for various Sn-butyl fragments grafted on silica surfaces allows concluding that this second complex is of the form (–Al–O)$_x$–Sn-(n-C_4H_9)$_{4-x}$ formed after substitution of x butyl groups by a corresponding number of bonds with surface oxygen atoms. The line width 2Γ of 0.76 mm/s of the doublet obtained for the (–Al–O)$_x$–Sn-(n-C_4H_9)$_{4-x}$ surface complex is very narrow, indicating that only a single species with a well-defined environment is formed rather than a multitude of complexes differing by their respective values of x.

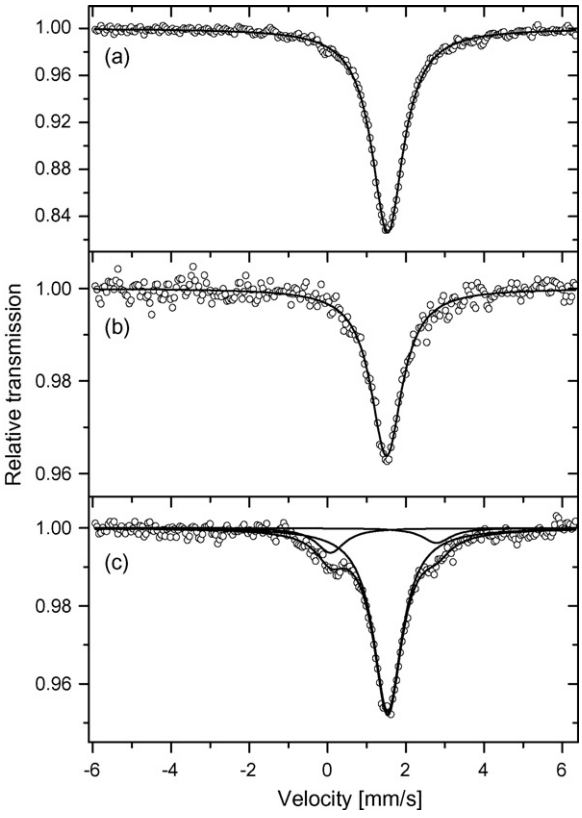

Fig. 1. Mössbauer spectra of (a) pure Sn-(n-C_4H_9)$_4$; (b) Sn-(n-C_4H_9)$_4$ adsorbed to deactivated alumina D and (c) Sn-(n-C_4H_9)$_4$ adsorbed to reactive alumina R. All spectra recorded at 16 K.

The interaction mechanisms between Sn-(n-C_4H_9)$_4$ and D and R alumina surfaces seen here are thus analogous to those observed previously for Pt(acac)$_2$. Hydroxylation of the alumina surface by an incipient wetness technique as described under (ii) in Section 2.1.1 does not lead to a complete surface

Table 1
^{119}Sn hyperfine parameters of some R-Sn-(n-C_4H_9)$_{4-x}$ complexes

Complex	δ (mm/s)	ΔE_q (mm/s)	T (K)	2Γ (mm/s)	Reference
Sn-(n-C_4H_9)$_4$	1.35[a]	0	80	[b]	[35]
Sn-(n-C_4H_9)$_4$	1.38[a]	0	77	[b]	[28]
Sn-(n-C_4H_9)$_4$	1.36	0	16	0.98	[c]
Sn-(n-C_4H_9)$_4$/Al_2O_3 (D)[d]	1.33	0	16	0.97	[c]
Sn-(n-C_4H_9)$_4$/Al_2O_3 (R)[d]	1.36	0	16	0.89	[c]
(–Al–O)$_2$–Sn-(n-C_4H_9)$_2$ (R)	1.27	2.72	16	0.76	
(≡Si–O)–Sn-(n-C_4H_9)$_3$	1.31[a]	2.50	77	[b]	[28]
(≡Si–O)$_2$–Sn-(n-C_4H_9)$_2$	1.23[a]	2.77	77	[b]	[28]
(≡Si–O)$_3$–Sn-(n-C_4H_9)	≈1.3[a]	≈2.6	77	[b]	[28]
O=Sn-(n-C_4H_9)$_2$	1.15[a]	2.08	80	1.56	[39]
HO–Sn-(n-C_4H_9)$_3$	1.37[a]	2.99	80	[b]	[40]
SnO_2	0.0–0.17	0.50–0.75	RT		[41–43]

δ: isomer shift with respect to $BaSnO_3$ at room temperature, ΔE_q: quadrupole splitting, T: temperature, 2Γ: full line width at half maximum.
[a] Isomer shift given with respect to SnO_2.
[b] Not reported.
[c] This work.
[d] Complex physisorbed to the alumina surface.

coverage by OH-groups [26]. The reactivity of the remaining c.u.s. surface sites of type A is, however, insufficient to allow a ligand exchange and formation of metal-oxygen bonds. Anchoring of Sn-(n-C_4H_9)$_4$ on deactivated alumina is limited to simple physisorption, in analogy to what was observed for Pt(acac)$_2$ [26]. The more reactive sites B on reactive alumina, resulting from calcination at 623 K, provide a sufficient number of neighbouring c.u.s. sites for substitution of x butyl groups of the tin complex by x surface oxygen atoms. In the case of Pt(acac)$_2$ we observed substitution of one acac-group of the platinum complex by at least two surface oxygen atoms [26,36]. The similarities in the behaviour of both the platinum and the tin complex towards alumina surfaces and a comparison of our Mössbauer parameters with those observed by Nédez et al. suggests that $x = 2$, *i.e.* substitution of two butyl groups by surface oxygen atoms.

It is worth noting that the doublet of this (–Al–O)$_2$–Sn-(n-C_4H_9)$_2$ complex is asymmetric with the left hand line being more intense than the right hand line, but with both lines of equal line width, indicating an anisotropy of the Mössbauer effect [37,38] and reflecting the inequivalence of the tin vibration modes parallel and perpendicular to the surface of the support, as it can be expected for surface-adsorbed molecules. We further note that no Mössbauer effect is observed at room temperature and only a very weak effect at liquid nitrogen temperature for both the physisorbed tetrabutyl and the (–Al–O)$_2$–Sn-(n-C_4H_9)$_2$ complex due to the absence of a rigid matrix around the tin atoms. We therefore recorded all spectra of surface complexes at 16 K, which reduced considerably the time necessary for data acquisition and allowed improved signal-to noise ratios.

3.2. Bimetallic $PtSn/Al_2O_3$ catalysts prepared by CSR

Platinum catalysts of various metal loadings and with various fractions of surface platinum atoms were used for the preparation of bimetallic samples as described in Section 2.1.2. Table 2a gives the metal loadings of the monometallic parent catalysts, the amount of tin contained in the solution used in the CSR step expressed in weight percent with respect to the support mass and as the atomic ratio Sn_0/Pt_s with respect to the number of surface platinum atoms determined by H_2/O_2 titration. It further indicates the atmosphere (Ar or H_2) under which the CSR was carried out. The result of the CSR is given in two forms, as the amount of tin effectively deposited in weight percent and also as an atomic ratio Sn/Pt_s with respect to the number of surface platinum atoms of the monometallic parent catalyst. Finally, the fraction of platinum surface atoms is given for both the initial monometallic and the final bimetallic catalyst. It can be noted that the amount of tin deposited is correlated with the number of surface platinum atoms Pt_s of the parent catalyst. The atomic ratio Sn/Pt_s is in all cases close to 0.5. No such correlation is seen with the initial tin concentration of the impregnation solution or with the initial atomic ratio Sn_0/Pt_s. This indicates that anchoring is limited to surface platinum atoms and that no interaction takes place between Sn-(n-C_4H_9)$_4$ and surface OH-groups. Thus, hydroxylation of the alumina surface in a moist gas stream prevents Sn-(n-C_4H_9)$_4$ very efficiently from anchoring on the surface of the support. Our Sn/Pts ratio of 0.5 is

Table 2
Characteristics of some $PtSn/Al_2O_3$ catalysts

Metal loading of parent catalyst (in wt.%)	Concentration of the impregnation solution (in wt.% Sn with respect to the support mass)	Initial ratio Sn atoms per Pt surface atoms Sn_0/Pt_s	Metal loading after deposition of Sn-(n-C_4H_9)$_4$ (in wt.%)	Ratio Sn atoms deposited per Pt surface atom Sn/Pt_s	Fraction of platinum surface atoms (in %) before and after deposition of tin
(a) Support hydroxylated					
Pt 0.25	0.13 (Ar)	1.04	Pt 0.25 Sn 0.06	0.48	83% → 72%
	0.13 (H_2)	1.04	Pt 0.25 Sn 0.06	0.48	83% → 70%
Pt 0.38	0.15 (Ar)	1.01	Pt 0.38 Sn 0.07	0.47	64% → n.d.
Pt 0.82	0.44 (Ar)	0.93	Pt 0.82 Sn 0.17	0.42	82% → n.d.
Pt 0.90	0.44 (Ar)	0.99	Pt 0.90 Sn 0.18	0.43	81% → 67%
Pt 1.15	0.56 (Ar)	1.48	Pt 1.15 Sn 0.25	0.69	54% → 55%
Pt 1.28	0.56 (Ar)	1.38	Pt 1.28 Sn 0.20	0.49	52% → 52%
Pt 1.48	0.72 (Ar)	1.78	Pt 1.48 Sn 0.18	0.45	45% → 47%
Pt 1.61	0.72 (Ar)	1.56	Pt 1.61 Sn 0.17	0.37	47% → 47%
Alumina	0.50 (H_2)		Sn 0.07		
(b) Support not hydroxylated					
Pt 0.46	n.d. (H_2)		Pt 0.46 Sn 0.58	2.5	83% → 63%

n.d.: not determined.

somewhat lower than the value of 0.8 observed in a previous study [18] which already emphasised the importance of surface hydroxylation, but used a less efficient method probably not eliminating all reactive surface sites.

A blank experiment on alumina, using a high concentration of Sn-(n-C_4H_9)$_4$, gives only a low amount of grafted tin, which might mainly result from some solution not eliminated by washing and remaining in the pores. With a pore volume to solution volume ratio of 0.6:5 (c.f. Section 2.1.2) a maximum of 12% of tin from the initial solution can remain in the pores and then be deposited on the support after evaporation of the solution. This corresponds in the case of the blank experiment to 0.06 wt.%, which agrees well with the 0.07 wt.% effectively found. This upper limit of 12% is further reduced when the tin concentration of the impregnation solution decreases during the CSR with platinum.

It can further be seen that the ratio Sn/Pt$_s$ is independent of the atmosphere under which the reaction is carried out. Providing additional hydrogen with the intention to facilitate the release of butyl groups by transformation to butane turned out to be without influence on the amount of tin anchored. With a Sn/Pts ratio of 0.5 the deposited tin atoms do not form a complete monolayer. As a consequence, the accessibility of platinum atoms is not fully reduced. The importance of the elimination of reactive sites on the support by hydroxylation is demonstrated by a CSR carried out on a platinum catalyst in the same way as described in Section 2.1.2, but without hydroxylation in a moist gas atmosphere. The surface sites on the support are those resulting from the final calcination at 623 K at the end of the platinum impregnation step and should thus be comparable to those on the reactive alumina described above. In this case the total number of tin atoms anchored exceeds by far the number of accessible surface platinum atoms. Despite this important amount of tin deposited the platinum dispersion remains at a high level of 63% (c.f. Table 2b). It must therefore be concluded that an important fraction of the tin complexes is anchored on the support.

The results demonstrate the importance elimination of both A and B sites has for successful preparations of second generation samples by CSR. It guarantees in the case of tin anchored on platinum a well-defined maximum Sn/Pt$_s$ ratio, which facilitates the preparation of PtSn/Al_2O_3 catalysts as the solution can to some extent be over-concentrated in tin. Complexes added to the solution in excess do not react with the support and are easily recovered at the end of the CSR step.

3.3. Analysis of a PtSn/Al_2O_3 catalyst

3.3.1. ^{119}Sn Mössbauer spectroscopy

The formation of the final PtSn/Al_2O_3 catalyst, Pt 0.90 wt.%, Sn 0.18 wt.%, was studied by ^{119}Sn Mössbauer spectroscopy at three stages of the drying and calcination procedure which follows the selective anchoring of Sn-(n-C_4H_9)$_4$ on reduced platinum: after drying at room temperature, after drying at 393 K and after calcination at 793 K. The spectra, all recorded at room temperature (298 K), are shown on Fig. 2b–d, respectively. A spectrum recorded at 16 K of the sample dried at room temperature is shown on Fig. 2a. The hyperfine parameters are gathered together in Table 3. The identification of the different phases observed in these spectra is based on an exhaustive study of the various tin species occurring in Sn/Al_2O_3 and SnPt/Al_2O_3 samples as a function of the preparation method or the oxidation and reduction conditions [33]. This study has revealed a large number of tin species, all differing in their specific hyperfine parameters δ (isomer shift) and ΔE_q (quadrupole splitting). It could, however, be shown that all these species can be grouped in a few categories on the basis of these parameters, and characteristic structural features could be associated with each of these categories. The various species observed in our present study will be grouped in these same categories as defined in Ref. [33] by their hyperfine parameters. A structural model of the bimetallic particles under study here will be proposed in the next section by making use of the structural features associated with each category in Ref. [33].

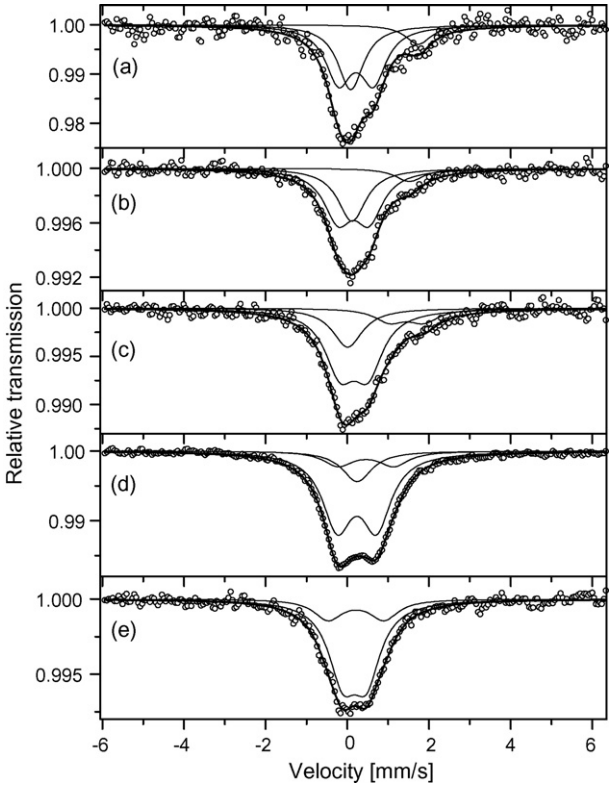

Fig. 2. Mössbauer spectra of a catalyst Pt 0.90 wt.% Sn 0.18 wt.% prepared by CSR of Sn(n–C_4H_9)$_4$ on reduced Pt/Al_2O_3: (a) sample dried at 298 K, spectrum recorded at 16 K; (b) sample dried at 298 K, spectrum recorded at 298 K; (c) sample dried at 393 K, spectrum recorded at 298 K; (d) sample calcined at 793 K, spectrum recorded at 298 K and (e) spectrum of a catalyst Sn 0.18 wt.% Pt 0.90 wt.% recorded at 298 K after calcination at 623 K.

Both the low temperature and the room temperature spectrum of the sample dried at 298 K (Fig. 2a and b) consist of three subspectra, a singlet and a doublet with isomer shifts close to zero and a singlet at $\delta = 1.56$ mm/s. The isomer shift of the first of these subspectra, labelled SnO_2 0 in Table 3, is typical for Sn^{4+} surrounded by an octahedron of oxygen atoms and lies in the range usually observed for bulk SnO_2. It differs, however, from the latter by its zero quadrupole splitting. According to

Table 3
^{119}Sn hyperfine parameters of a $PtSn/Al_2O_3$ catalyst after various stages of the final drying procedure

Drying temperature (K)	δ (mm/s)	ΔE_q (mm/s)	2Γ (mm/s)	C (%)	Identification
298[a]	−0.09	0	0.77	34	SnO_2 0
	0.02	0.86	0.77	56	SnO_2 1 or Sn^{IV} 2
	1.56	0	0.77	10	Pt_xSn
298[b]	−0.07	0	0.85	33	SnO_2 0
	−0.03	0.76	0.85	59	SnO_2 1 or Sn^{IV} 2
	1.35	0	0.85	8	Pt_xSn
393[b]	−0.17	0	0.89	22	SnO_2 0
	−0.02	0.70	0.89	64	SnO_2 1 or Sn^{IV} 2
	1.29	0.83	0.89	14	$Pt_xSn(O)$
793[b]	0.06	0	0.88	15	SnO_2 0
	0.05	0.96	0.88	71	Sn^{IV} 2
	0.28	1.36	0.88	14	Sn^{IV} 2

δ: isomer shift with respect to $BaSnO_3$ at room temperature, ΔE_q: quadrupole splitting, 2Γ: full line width at half maximum, C: relative contribution to the total absorption.
[a] Spectrum recorded at 16 K.
[b] Spectrum recorded at 298 K.

Ref. [33] this species corresponds to small, rather molecule-like clusters on the outermost sphere of a particle. Due to the weak interactions with surrounding atoms, the Sn–O bonds are free of strain and relax to form a perfect octahedron as reflected by the zero quadrupole splitting. The second species, with a quadrupole splitting at the upper limit of the typical range observed for bulk SnO_2, can be attributed to either tin atoms in bulk-SnO_2-like clusters (labelled SnO_2 1 in Ref. [33]) or to tin atoms in contact with another metal via bridging oxygen atoms, like Sn–O–Al or Sn–O–Pt, which leads to a stronger asymmetry of the chemical bonds in the SnO_6-cluster than in the bulk material and thus to an increased quadrupole splitting (labelled Sn^{IV} 2 in Ref. [33]). We leave here open whether this species is rather bulk SnO_2 or influenced by interactions with the support or platinum and label it SnO_2 1/Sn^{IV} 2 in Table 3. We shall return to this point in the next section. It can be noted that the isomer shifts of these first two subspectra are clearly different from that of Sn-(n-C_4H_9)$_4$ reflecting the total decomposition of the anchored tin alkyl complex and the complete oxidation of the tin atoms upon prolonged contact with air. A corresponding observation of rapid oxidation upon contact with air was reported by Vértes et al. for Sn-(C_2H_5)$_4$ deposited by CSR on reduced platinum [32]. The hyperfine parameters of the third subspectrum are similar to those of Sn-(n-C_4H_9)$_4$ and could, at first glance, be attributed to Sn-(n-C_4H_9)$_4$ physisorbed to the support. However, the corresponding subspectrum appears in both the room temperature and the low temperature spectrum with almost identical relative intensities, in contrast to the observation that adsorbed Sn-(n-C_4H_9)$_4$-complexes reveal no Mössbauer effect at room temperature (c.f. Section 3.1). We therefore attribute this spectrum to a platinum-rich alloy of the Pt_3Sn-type, for which isomer shifts between 1.4 and 1.7 mm/s and zero quadrupole splittings were reported [19,42,44,45]. Tin atoms completely surrounded by platinum could result from the aforementioned sintering of the platinum particles during the selective anchoring of the tin complexes. The relative spectral intensities of the three species show that only a minor fraction of the tin atoms is enclosed in such a platinum matrix and that by far the majority of all tin atoms is present in oxidised form. A similar result was obtained by Millet et al. [22] for $RhSn/SiO_2$ catalysts prepared by a CSR method similar to ours, where a minor fraction of tin is found in form of a rhodium-rich alloy and the majority of tin situated on the surface of the rhodium particles.

Drying at 393 K does not alter the two forms of oxidised tin. The spectrum of the metallic form, however, now clearly reveals a quadrupole splitting, while its isomer shift remains close to the typical domain of PtSn alloys. Such hyperfine parameters were also observed in Ref. [33] after reoxidation of the reduced particles of PtSn catalysts and were attributed to the formation of an "oxometallic" $Pt_xSn(O)$ species, in which the Pt_xSn particle is in contact with one or several oxygen atoms at its surface. Calcination at 793 K finally completely oxidises these metallic particles. The high quadrupole splitting clearly distinguishes them from bulk-like SnO_2 and indicates an interaction with neighbouring Pt atoms via Sn–O–Pt bridges. Consequently, this phase is now considered as Sn^{IV} 2. The final calcination has also modified the SnO_2 1/Sn^{IV} 2 phase. Its quadrupole splitting has increased to 0.94 mm/s and lies now above the typical SnO_2 values and well within the range defined in Ref. [33] for Sn^{IV} 2. Apparently, the calcination has created Sn–O–metal bridges or strengthened such bonds already existing before. The SnO_2 0 species remains unaffected by this calcination.

3.3.2. Structural model

This section will attempt to develop a structural model of the various tin species – SnO_2 0, SnO_2 1/Sn^{IV} 2, Pt_xSn and $Pt_xSn(O)$ – distinguished in the Mössbauer spectra. We will take into account some results of Merlen et al. who analysed $PtSn/Al_2O_3$ catalysts prepared by a CSR method very similar to ours [46] by a number of techniques like X-ray energy dispersive spectrometry (XEDS), low energy ion scattering (LEIS) and transmission electron microscopy (TEM). The results showed that the surface of the particles is mainly composed of tin atoms. Progressive ablation of the outermost atomic shell by the inci-

dent He^+ beam in the LEIS experiment increased the fraction of surface platinum atoms. Analysis of the composition of individual particles by XEDS showed that their Pt/Sn atomic ratio increased with particle size, which also agrees with a morphology in which the bulk of the particles is mainly composed of platinum atoms while tin atoms form a surface layer.

When interpreting our Mössbauer spectra in terms of tin anchoring sites we must take into account the particle size distribution of the monometallic parent catalyst. In Ref. [26] we have shown by TEM that the size distribution of such a high dispersion catalyst is extremely narrow with 88% of the TEM-detectable particles in the 0.7–1.2 nm size range, which means a particle diameter of three to five atoms if we take 0.276 nm as the Pt atomic diameter. For such small particles three kinds of anchoring sites can be imagined. The first is next to a platinum atom on the support (Fig. 3a, atom labelled 1), with hydrogen atoms from the hydroxylated alumina surface facilitating the release of all butyl groups. The second is attached to the surface of the particle, for example on its top (atom 2). The Sn atoms on Fig. 3a are shown surrounded by oxygen atoms to take into account their reoxidation in air revealed by Mössbauer spectroscopy. Tin atom 1 is surrounded by six oxygen atoms some of which are part of the support and some are connected to platinum. This diversity of bonds causes some distortion of the SnO_6-octahedron giving rise to a non-zero quadrupole splitting in the Mössbauer spectrum. We therefore associate this situation with the SnO_2 1/Sn^{IV} 2 species from Table 3. SnO_6-octahedra connected to the surface of a particle by a low number of bonds (atom 2) are able to better conserve their ideal octahedral symmetry, resulting in a zero quadrupole splitting. We thus identify the SnO_2 0 species seen in the Mössbauer spectra with such surface atoms. A third possibility is shown on Fig. 3b: a tin atom enclosed by platinum (atom 3). Such a situation can either be the result of sintering, with a tin atom originally situated on the surface of a particle and then enclosed by coalescence of two neighbouring particles, or can result from direct anchoring deep inside a platinum particle in a kind of stacking default, occupying the place of a missing platinum atom. Enclosed in this way, the tin atom is prevented from oxidation in air and adopts a rather metallic state. We associate the Pt_xSn species with such an enclosed tin atom like in Fig. 3b.

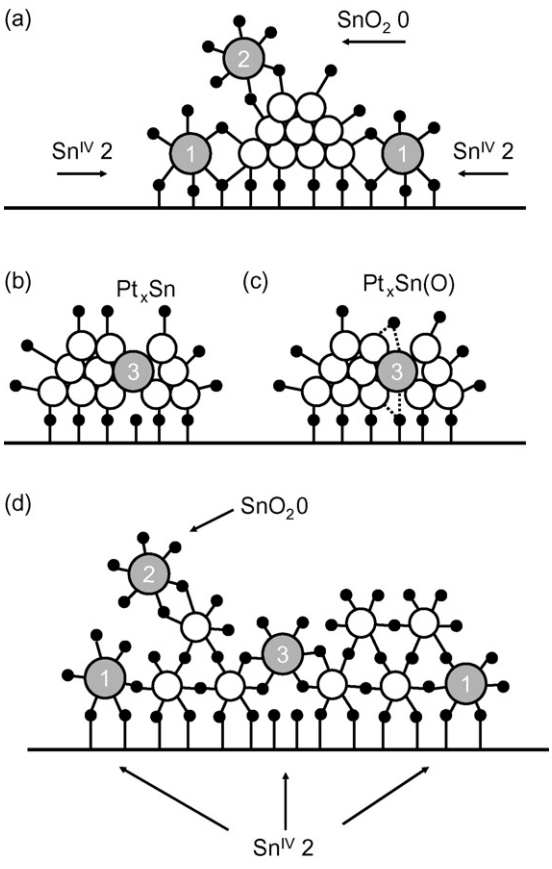

Fig. 3. Schematic representation of tin anchoring sites on Pt particles: (a and b) after deposition of $SnBu_4$ on reduced platinum and prolonged contact with air at 298 K; (c) after drying at 393 K and (d) after calcination at 793 K. White: Pt, grey: tin; black: oxygen.

Drying at 393 K modifies only the metallic Pt_xSn form. According to Ref. [33] the appearance of a quadrupole splitting while maintaining an isomer shift typical for Pt_xSn alloys can be explained by either the presence of a bridging oxygen atom, situated above the tin and a neighbouring platinum atom, or by enhanced interaction with a surface oxygen atom from the support. Both possibilities are shown on Fig. 3c by dashed lines to indicate two alternative situations leading to a $Pt_xSn(O)$ species.

Calcination at 793 K transforms metallic platinum into a PtO_2-like particle as was demonstrated by X-ray absorption spectroscopy [36]. The tin atom embedded in the platinum particle (atom 3 on Fig. 3b and c) is now completely oxidised. The different ionic radii of Pt^{IV} and Sn^{IV} might be responsible for a deformation of the angles of the bridging Sn–O–Pt bonds which form the SnO_6-octahedron, leading in this way to an important quadrupole splitting in the Mössbauer spectrum clearly different from what is generally observed for bulk SnO_2. The species is therefore now classified as Sn^{IV} 2 (Fig. 3d). The volume expansion accompanying the oxidation process modifies also the environment of the tin atoms situated on the support and attached to platinum particles (atom 1 on Fig. 3a) causing stronger deformations of their SnO_6-octahedra and thus an increase of the quadrupole splitting as compared to the initial situation of Fig. 3a. The Mössbauer parameters of this species are now clearly different from those of bulk SnO_2 justifying our hypothesis of a tin species in contact with the surface of the support and a platinum particle. Consequently we classify it now also as Sn^{IV} 2. Only SnO_6-octahedra attached to the platinum particle by a minimum number of bonds (atom 2) remain unaffected by the calcination and conserve their high symmetry as reflected by the zero quadrupole splitting.

It follows from this model and from the relative intensities of the Mössbauer subspectra of these three types of tin atoms that an important amount of tin is situated next to a platinum particle on the support and only a minor fraction on the surface of a particle. This would explain the fact that the accessibility of the platinum atoms measured by H_2/O_2 titration is unaffected by the deposition of tin. We emphasize the appearance of a metallic form of tin, the Pt_xSn alloy, which is a direct proof that tin has been anchored directly on a platinum particle.

Table 4
^{119}Sn hyperfine parameters of $PtSn/Al_2O_3$ and $SnPt/Al_2O_3$ catalysts

Sample	δ (mm/s)	ΔE_q (mm/s)	2Γ (mm/s)	C (%)	Identification
Sn 0.54[a]	0.00	0.00	0.82	23	SnO_2 0
	0.04	0.83	0.82	77	Sn^{IV} 2
Sn 0.51 Pt 0.33[a]	0.06	0.53	0.82	68	SnO_2 1
	0.11	1.12	0.82	32	Sn^{IV} 2
Sn 0.18 Pt 0.90[b]	0.00	0.59	0.86	78	SnO_2 1
	0.04	1.34	0.86	22	Sn^{IV} 2
Pt 0.90 Sn 0.18[b]	0.06	0.00	0.88	15	SnO_2 0
	0.05	0.96	0.88	71	Sn^{IV} 2
	0.28	1.36	0.88	14	Sn^{IV} 2

δ: isomer shift with respect to $BaSnO_3$ at room temperature, ΔE_q: quadrupole splitting, 2Γ: full line width at half maximum, C: relative contribution to the total absorption. All spectra recorded at room temperature.
[a] Ref. [33].
[b] This work.

3.4. Comparison of $PtSn/Al_2O_3$ and $SnPt/Al_2O_3$ catalysts

The catalyst described in the previous section, Pt 0.90 wt.%, Sn 0.18 wt.%, is now compared to a catalyst of identical metal loading, but with the two metals deposited in the inverse order, Sn 0.18 wt.%, Pt 0.90 wt.%, as described in Section 2.1.3. The preparation method chosen for the latter does not include a CSR step for the deposition of the second metal. Platinum should therefore be anchored directly on the support, eventually to some extent next to and in contact with tin particles. The room temperature spectrum of the $SnPt/Al_2O_3$ catalyst recorded after the final calcination at 623 K is shown on Fig. 2e. Table 4 compares the hyperfine parameters of the two catalysts. Included in this table are a monometallic sample and the corresponding bimetallic catalyst from Ref. [33], prepared in the same way as described in Section 2.1.3. The comparison with these two samples helps to understand the evolution the tin particles undergo during the platinum anchoring step. The Mössbauer spectrum of the monometallic sample, Sn 0.54 wt.%, consists of two subspectra, a singlet of the SnO_2 0 phase and a doublet of a Sn(IV) oxide where tin is in contact with the support via Sn–O–Al bridges. The major part of the tin atoms belongs to this latter phase, reflecting the direct anchoring of the metal on the surface of the support, while the SnO_2 0 species might represent single SnO_6-cluster placed on top of an agglomerate of Sn^{IV} 2. After impregnation with platinum (Sn 0.51 wt.%, Pt 0.33 wt.%) only a minor fraction of the tin atoms remains in contact with another metal (Al or Pt) in the form of a Sn^{IV} 2 species while the majority has been transformed to a SnO_2-like phase labelled SnO_2 1 the hyperfine parameters of which agree well with those of bulk SnO_2. These changes indicate that (i) only a small fraction of the platinum was anchored next to tin particles and (ii) a sintering of the tin particles occurs during the platinum impregnation procedure leading to larger agglomerates of tin and oxygen atoms, which adopt a bulk-SnO_2-like structure. In this way the fraction of tin atoms in contact with the support is strongly reduced.

The spectrum of the SnPt catalyst prepared in this work shows the same two phases with similar hyperfine parameters and in similar proportions. It is obvious that the formation of larger agglomerates of tin oxide is rather undesired since all tin enclosed inside such clusters is prevented from contact with platinum and thus inactive in view of an improvement of the catalytic performances of the sample. The SnPt-catalyst differs insofar from the corresponding PtSn-sample as in the latter the majority of tin is in contact with another metal, either via oxygen bridges or directly by formation of a Pt_xSn phase.

4. Conclusion

The interaction between Sn-(n-C_4H_9)$_4$ and alumina surfaces is governed by three types of surface sites: surface OH-groups and two kinds of c.u.s. surface sites of different reactivity. We observed no interaction with, and no anchoring on, OH groups, physisorption on the less reactive and partial decomposition of the complex on the more reactive of the two c.u.s. sites. These three different interaction mechanisms are identical to those observed previously for the platinum precursor Pt(acac)$_2$.

Elimination of all reactive sites allows the controlled preparation of bimetallic $PtSn/Al_2O_3$ catalysts by selective anchoring of the tin complex on reduced metal particles of a Pt/Al_2O_3 parent catalyst, avoiding undesired anchoring of tin on the support.

The morphology of the bimetallic particles is analysed on an atomic scale by ^{119}Sn Mössbauer spectroscopy. Evidence was found that the majority of tin is situated on the support in contact with a platinum particle, minor fractions are deposited on the particle surface or are enclosed inside a particle in form of an alloy. No evidence was found for the formation of bulk-SnO_2-like agglomerates in which an important amount of tin would be enclosed inside, isolated from platinum particles, and thus inactive in view of an improvement of the catalytic performances of the sample. In contrast to this the preparation of a bimetallic catalyst without making use of a controlled surface reaction, led to important amounts of bulk SnO_2 and only a minor fraction of tin in contact with platinum.

References

[1] F.M. Dautzenberg, German Patent 2,121,765, 1971.
[2] F.M. Dautzenberg, German Patent 2,153,891, 1972.
[3] F.C. Wilhelm, US Patent 3,844,938, 1974.
[4] N. Macleod, J.R. Fryer, D. Stirling, G. Webb, Catal. Today 46 (1998) 37–54.
[5] M.C. Rangel, L.S. Carvalho, P. Reyes, J.M. Parera, N.S. Figoli, Catal. Lett. 64 (2000) 171–178.
[6] Z. Poltarzewski, S. Galvagno, R. Pietropaola, P. Staiti, J. Catal. 102 (1986) 190–198.
[7] F. Coloma, A. Sepulveda-Escribano, J.L.G. Fiero, F. Rodriguez-Reinoso, Appl. Catal. A 148 (1996) 63–80.
[8] G. Neri, C. Milone, S. Galvagno, A.J.P. Pijpers, J. Schwank, Appl. Catal. A 227 (2002) 105–115.
[9] V.N. Seleznev, Y.V. Formichev, M.E. Levinter, Neftekhimiya 14 (1974) 205–212.
[10] F.M. Dautzenberg, J.N. Helle, P. Biloen, W.M.H. Sachtler, J. Catal. 63 (1980) 119–128.
[11] P. Biloen, J.N. Helle, H. Verbeek, F.M. Dautzenberg, W.M.H. Sachtler, J. Catal. 63 (1980) 112–118.
[12] J. Burch, J. Catal. 71 (1981) 348–359.
[13] G.T. Baronetti, S.R. de Miguel, O. Scelza, M.A. Fritzler, A.A. Castro, Appl. Catal. 19 (1985) 77–85.

[14] Y. Zhou, S.M. Davies, Catal. Lett. 15 (1992) 51–55.
[15] J.L. Margitfalvi, M. Hegedüs, S. Göbölös, E. Kern-Tàlas, P. Szedlacsek, S. Szabö, Proceedings of the Eighth International Congress on Catalysis, vol. 4, Verlag Chemie (Weinheim), Berlin, 1984, pp. 903–914.
[16] C. Travers, J.P. Bournonville, G. Martino, Proceedings of the Eighth International Congress on Catalysis, vol. 4, Verlag Chemie (Weinheim), Berlin, 1984, pp. 891–902.
[17] J.L. Margitfalvi, I. Borbáth, J. Mol. Catal. A 202 (2003) 313–326.
[18] F. Bentahar, F. Bayard, J.P. Candy, J.M. Basset, B. Didillon, in: J.P. Blitz, C.B. Little (Eds.), Fundamental and Applied Aspects of Chemically Modified Surfaces, RCS publ, 1999, pp. 235–245.
[19] J.P. Candy, B. Didillon, E.L. Smith, T.B. Shay, J.M. Basset, J. Mol. Catal. 86 (1994) 179–204.
[20] F. Humblot, B. Didillon, F. Le Peltier, J.P. Candy, J. Corker, O. Clause, F. Bayard, J.M. Basset, J. Am. Chem. Soc. 120 (1998) 137–146.
[21] J.L. Margitfalvi, I. Borbáth, M. Hegedüs, A. Tompos, Appl. Catal. A 229 (2002) 35–49.
[22] J.M.M. Millet, J. Toyir, B. Didillon, J.P. Candy, C. Nédez, J.M. Basset, Hyperfine Interact. 108 (1997) 477–482.
[23] J.B. Peri, J. Phys. Chem. 69 (1965) 220–230.
[24] H. Knözinger, P. Ratnasamy, Catal. Rev. Sci. Eng. 17 (1978) 31–70.
[25] H. Knözinger, Adv. Catal. 25 (1976) 184–271.
[26] M. Womes, T. Cholley, F. Le Peltier, S. Morin, B. Didillon, N. Szydlowski-Schildknecht, Appl. Catal. A 283 (2005) 9–22.
[27] C. Nédez, A. Theolier, F. Lefebvre, A. Choplin, J.M. Basset, J.F. Joly, J. Am. Chem. Soc. 115 (1993) 722–729.
[28] C. Nédez, F. Lefebvre, A. Choplin, J.M. Basset, E. Benazzi, J. Am. Chem. Soc. 116 (1994) 3039–3046.
[29] J.L. Margitfalvi, I. Borbáth, M. Hegedüs, S. Göbölös, F. Lonyi, React. Kinet. Catal. Lett. 68 (1999) 133–143.
[30] J.L. Margitfalvi, I. Borbáth, M. Hegedüs, S. Göbölös, A. Tompos, F. Lonyi, in: A. Corma, F.V. Melo, S. Mendioroz, J.L.G. Fierro (Eds.), Proceedings of the 12th International Congress on Catalysis, Granada, 2000, Stud. Surf. Sci. Catal., vol. 130, part B, Elsevier (Amsterdam) 2000, pp. 1025–1030.
[31] J.L. Margitfalvi, I. Borbáth, E. Tfirst, A. Tompos, Catal. Today 43 (1998) 29–49.
[32] C. Vértes, E. Tálas, I. Czakó-Nagy, J. Ryczkowski, S. Göbölös, A. Vértes, J.L. Margitfalvi, Appl. Catal. 68 (1991) 149–159.
[33] J. Olivier-Fourcade, M. Womes, J.C. Jumas, F. Le Peltier, S. Morin, B. Didillon, ChemPhysChem 5 (2004) 1734–1744.
[34] W. Kündig, Nucl. Instr. Methods 75 (1969) 336–340.
[35] A.G. Davies, J.A.A. Hawari, J. Organomet. Chem. 201 (1980) 221–231.
[36] M. Womes, J. Lynch, D. Bazin, F. Le Peltier, S. Morin, B. Didillon, Catal. Lett. 85 (2003) 25–31.
[37] V.I. Goldanskii, E.F. Makarov, V.V. Khrapov, Phys. Lett. 3 (1963) 344–346.
[38] S.V. Karyagin, Proc. Acad. Sci. USSR, Phys. Chem. Sect. 148 (1964) 110.
[39] T.C. Gibb, N.N. Greenwood, J. Chem. Soc. A (1966) 43–46.
[40] J.M. Brown, A.C. Chapman, R. Harper, D.J. Mowthorpe, A.G. Davies, P.J. Smith, J. Chem. Soc. Dalton Trans. (1972) 338–341.
[41] Y.X. Li, K.J. Klabunde, B.H. Davis, J. Catal. 128 (1991) 1–12.
[42] V.I. Kuznetzov, A.S. Belyie, E.N. Yurchenko, M.D. Smolikov, M.T. Protasovan, E.V. Zatolokina, V.K. Duplyakin, J. Catal. 99 (1986) 159–170.
[43] J.J. Zuckerman, in: E.H. Herbert (Ed.), Chemical Mössbauer Spectroscopy, Plenum Press, New York, London, 1984, pp. 267–293.
[44] R. Srinivasan, R. Sharma, S. Su, B.H. Davis, Catal. Today 21 (1994) 83–99.
[45] V.I. Kuznetsov, E.N. Yurtchenko, in: Yu.M. Kagan, I.S. Lyubutin (Eds.), Applications of the Mössbauer Effect, Gordon and Breach Science Publishers, 1985, pp. 1155–1158.
[46] E. Merlen, P. Beccat, J.C. Bertolini, P. Delichère, N. Zanier, B. Didillon, J. Catal. 159 (1996) 178–188.